

Effects of Sr doping on the optical properties of polycrystalline $\text{La}_{2-x}\text{Sr}_x\text{CuO}_{4-y}$

G. L. Doll and J. T. Nicholls

Department of Physics, Massachusetts Institute of Technology, Cambridge, Massachusetts 02139

M. S. Dresselhaus

Departments of Physics and Electrical Engineering and Computer Science, Massachusetts Institute of Technology, Cambridge, Massachusetts 02139

A. M. Rao, J. M. Zhang, G. W. Lehman, and P. C. Eklund

Department of Physics and Astronomy, University of Kentucky, Lexington, Kentucky 40506

G. Dresselhaus

Francis Bitter National Magnet Laboratory, Massachusetts Institute of Technology, Cambridge, Massachusetts 02139

A. J. Strauss

Lincoln Laboratory, Massachusetts Institute of Technology, Lexington, Massachusetts 02173

(Received 16 May 1988; revised manuscript received 8 August 1988)

We have measured the room-temperature near-normal-incidence reflectivity of polycrystalline pellet samples of $\text{La}_{2-x}\text{Sr}_x\text{CuO}_{4-y}$ with $x=0, 0.05, 0.10, 0.15,$ and 0.20 over a wide frequency range ($100\text{--}50000\text{ cm}^{-1}$). The reflectance data have been fitted by an effective-medium approximation that takes into account the anisotropy in the dielectric functions perpendicular and parallel to the CuO_2 planes. Results of our analysis concerning the optical properties of the CuO_2 planes agree with reflectance data recently reported by Tajima *et al.* for the $E \perp \hat{c}$ polarization spectrum of single-crystal $\text{La}_{1.83}\text{Sr}_{0.17}\text{CuO}_{4-y}$. In addition to the frequencies and symmetries of the ir-active phonons, the plasmons of the system have been studied systematically as a function of Sr concentration.

I. INTRODUCTION

To date, no analysis of the optical properties of polycrystalline $\text{La}_{2-x}\text{Sr}_x\text{CuO}_{4-y}$ that specifically incorporates the important ir anisotropy has been presented systematically as a function of x . In this study, we have measured the room-temperature near-normal-incidence reflectance spectra of $\text{La}_{2-x}\text{Sr}_x\text{CuO}_{4-y}$ for x in the range $0 \leq x \leq 0.20$, which includes the composition range of the highest T_c values for this system. The large spectral range covered by the present work ($100\text{ cm}^{-1} < \omega < 50000\text{ cm}^{-1}$) allows analysis of the x dependence of the ir phonons and plasmons. By using elementary effective-medium theory to fit the spectra, we have extracted the symmetries and frequencies of the ir-active in-plane (E_u) and out-of-plane (A_{2u}) vibrations through comparative analysis with isostructural materials, and have obtained the ab -plane Drude parameters as a function of x .

In the past year, numerous optical experiments have been reported on the high- T_c cuprate $\text{La}_{2-x}\text{Sr}_x\text{CuO}_{4-y}$. Many of these studies have focused on the optical properties of Sr-doped polycrystalline La_2CuO_4 .¹⁻¹² The measured optical properties were analyzed in some cases^{1,11} by Kramers-Kronig transform techniques although the optical properties of $\text{La}_{2-x}\text{Sr}_x\text{CuO}_{4-y}$ are known to be highly anisotropic.⁶ The significance of the effects of the anisotropy on the polycrystalline reflectance data of $\text{La}_{2-x}\text{Sr}_x\text{CuO}_{4-y}$ materials became apparent following a polarized reflectance study of an isomorphous La_2NiO_4 sin-

gle crystal by Bassat, Odier, and Gervais.¹³ They reported that the spectrum of the insulating \hat{c} direction ($E \parallel \hat{c}$) consisted of two very strong reststrahlen bands, while the spectrum of the ab planes ($E \perp \hat{c}$) exhibited phonon structure superimposed on an overdamped Drude response. The results of the La_2NiO_4 study were found to apply to the La_2CuO_4 system following a reflectivity study performed on the c face of a superconducting single crystal of $\text{La}_{1.8}\text{Sr}_{0.2}\text{CuO}_4$ reported by Tajima and co-workers,¹⁴ who found the spectrum of the CuO_2 planes to be metallic and well described by Drude theory. By comparing their single-crystal data to spectra obtained from randomly oriented polycrystalline grains, they constructed the reflectivity spectrum for the $E \parallel \hat{c}$ polarization and found it remarkably similar to the out-of-plane spectrum reported for La_2NiO_4 .

II. EXPERIMENTAL DETAILS

The polycrystalline samples were prepared by standard ceramic techniques. Powders of La_2O_3 , SrCO_3 , and CuO were combined in appropriate proportions to prepare mixtures with the desired compositions. These mixtures were fired in air at 1000°C for two periods of 18 h each, with an intermediate grinding. Each sample was then re-ground and pressed at about 15000 psi to form cylindrical pellets ~ 2 cm in diameter and $\sim \frac{1}{2}$ cm thick. The pellets were fired in air at 1000°C for 16 h, cooled to room temperature, then refired for 144 h. Finally, they were fired

at 900°C in flowing N₂ for 2 h and at 500°C in flowing O₂ for 3 h, then cooled to room temperature at 1°C/min. All firings were carried out in Pt crucibles. Powder x-ray diffraction data showed the final samples to be single phase, with either the K₂NiF₄ tetragonal structure ($x \geq 0.10$) or an orthorhombic distortion of the tetragonal structure ($x \leq 0.05$). (The N₂ firing was used to remove traces of a second phase from the tetragonal samples.)

The microstructure of the ceramic pellets was examined by scanning electron microscopy (SEM) and Auger electron spectroscopy performed in a Perkin Elmer PHI 661 scanning Auger multiprobe system. Rectangular pieces (5×5×10 mm³) were cut from the pellets and fractured in the system under high-vacuum conditions (2×10⁻¹⁰ Torr) to avoid surface contamination. SEM micrographs revealed equiaxed grains with approximate dimensions of 5–10 μm. A relatively homogeneous distribution of La, Cu, and O was observed throughout the examined region, but there was evidence of some Sr segregation at the grain boundaries. This segregation effect has been addressed elsewhere.¹⁵

As a further characterization, ac-susceptibility measurements were performed to determine the superconducting transition temperatures of the samples. In the temperature range examined ($T > 4$ K), no transition was observed for the $x = 0$ and 0.05 samples, while transitions with onsets at 29, 40, and 37 K were observed for the $x = 0.10, 0.15,$ and 0.20 samples, respectively. These values are in good agreement with other published data on polycrystalline La_{2-x}Sr_xCuO_{4-y}.¹⁶

Optical reflectance measurements were performed in a near-normal-incidence configuration using a Digilab FTS-80 interferometer (80–4000 cm⁻¹) and a Perkin Elmer Model 88 prism monochromator (0.1–4.0 eV). To minimize the effect of surface roughness, the reflectance was first measured on the as-prepared sample. The sample was then coated with an evaporated Al film about 1000 Å thick, and the reflectance was measured versus an Al film. The reflectance spectra shown in this work represent the quantity $R(\omega) = R_s(R_{Al}/R_{s,Al})$, where R_s , R_{Al} , and $R_{s,Al}$ are, respectively, the near-normal reflectance of the uncoated sample, aluminum mirror, and Al overcoated sample.

III. RESULTS AND DISCUSSION

A. Anisotropy model

The room-temperature reflectance spectra of polycrystalline ceramic samples of La_{2-x}Sr_xCuO_{4-y} with $x = 0, 0.05, 0.10, 0.15,$ and 0.20 are shown in Fig. 1. Inspection of the spectra reveals a quite complicated arrangement of infrared spectral features and a significant departure from classical Drude response. Previous work⁹ on the optical properties of La_{1.85}Sr_{0.15}CuO_{4-y} suggests that the ir anisotropy of the La_{2-x}Sr_xCuO_{4-y} system can be modeled using elementary effective-medium theory. The reflectivity spectra were modeled following the procedure outlined

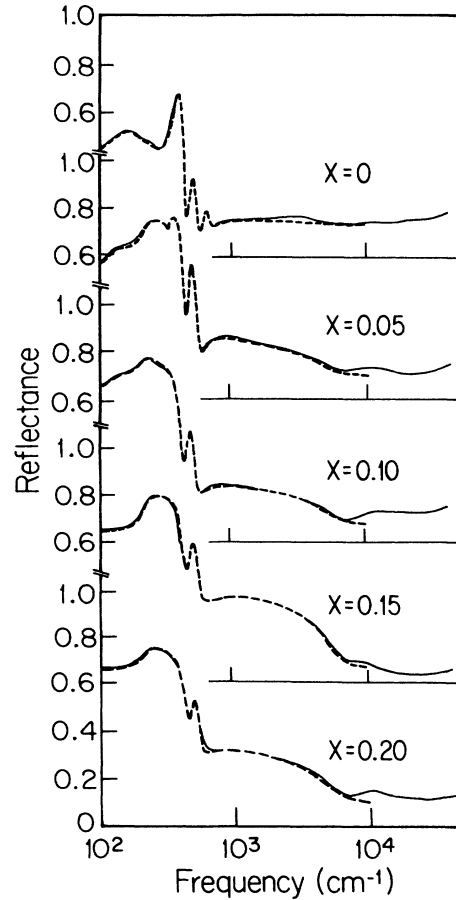


FIG. 1. Reflectance spectra of La_{2-x}Sr_xCuO_{4-y} taken at room temperature in a near-normal-incidence geometry. The dashed lines are fits to the data using the effective-medium anisotropy model given in Eq. (1). The optical parameters of the fits are gathered in Table I. The normal-mode eigenvectors shown schematically in the figure are appropriate to K₂MnF₄ (Ref. 21) and a force-constant model is required to find the appropriate modes for La₂CuO₄.

in Ref. 8 as

$$R(\omega) = (f)R_{\perp}(\omega) + (1-f)R_{\parallel}(\omega), \quad (1)$$

where R_{\perp} and R_{\parallel} are the reflectances of faces \perp and \parallel to the crystallographic \hat{c} axis, and f is the volume fraction of the R_{\perp} component. For tetragonal symmetry, $f = \frac{2}{3}$. In this work the \hat{c} axis is taken as the crystallographic axis of uniaxial symmetry, which is perpendicular to the CuO₂ planes. The values of R_{\perp} and R_{\parallel} were obtained by modeling the dielectric functions from the factorized form of the dielectric function¹⁷

$$\frac{\epsilon(\omega)}{\epsilon_{\infty}} = \prod_j \frac{\Omega_{j,LO}^2 - \omega^2 \pm i\omega\gamma_{j,LO}}{\Omega_{j,TO}^2 - \omega^2 \pm i\omega\gamma_{j,TO}} - \frac{\omega_p^2}{\omega(\omega + i\gamma_p)}, \quad (2)$$

and by adjusting Ω_j , γ_j , ω_p , and γ_p , which represent the longitudinal optical (LO) and transverse optical (TO) phonon frequencies, their damping factors, the plasma frequency, and its damping constant, respectively. After $\epsilon_{\perp}(\omega)$ and $\epsilon_{\parallel}(\omega)$ were calculated from Eq. (2), $R_{\perp}(\omega)$

and $R_{\parallel}(\omega)$ were obtained in the standard way,¹⁸ and then substituted in Eq. (1), yielding the composite reflectivity $R(\omega)$.

Fits of Eq. (1) to the data are shown as dashed lines in Fig. 1 and describe the data very well over a wide frequency range. The discrepancy between the calculated and experimental values above $\sim 6500 \text{ cm}^{-1}$ is attributed to the onset of interband transitions above the plasma frequency, which were not considered in our calculations. The low-frequency regions of the spectra are rich in structure associated with ir phonons, the symmetries and frequency assignments of which are addressed in the next section. Values of the fitting parameters are listed in Table I for the different Sr concentrations studied.

Table II lists the optical parameters of the $x=0.15$ composition deduced in this work and in previous studies on polycrystalline ceramic samples by Sulewski, Noh, McWhirter, and Sievers⁷ and Schlesinger, Collins, Shafer, and Engler⁸ together with the parameters obtained by Tajima *et al.*¹⁴ from data for the c face (ab planes) of a single crystal of $\text{La}_{1.83}\text{Sr}_{0.17}\text{CuO}_{4-y}$. The values of Sulewski *et al.* and Schlesinger *et al.* were derived from other anisotropy models. While the TO and LO phonon frequencies are similar for the three polycrystalline studies, disagreement is found between the values of the Drude parameters ω_p , γ_p , and ϵ_{∞} . Since the spectrum of our $x=0.15$ sample is essentially identical with the spectra reported in Refs. 7 and 8, we conclude that evaluation of the Drude parameters of the ceramic samples is model dependent. Due to the composite nature of these materials and the approximations used in the anisotropy models of this and other studies,^{7,8} it is not possible

to obtain reliable absolute values for the Drude parameters (ϵ_{∞} , ω_p , γ_p). However, since the reflectivity spectra reported here were obtained from a sample set with similar morphologies and since these spectra were fit within the same model, we have confidence in the reliability of the relative x dependence of the fitting parameters. A fully reliable determination of the Drude parameters of $\text{La}_{2-x}\text{Sr}_x\text{CuO}_4$ can only be obtained from single-crystal spectra; however, homogeneous Sr-doped single crystals have proven difficult to synthesize. Therefore the development of an anisotropy model for the polycrystalline cuprates which comes closest to reproducing the single-crystal results is of great importance.

B. Infrared phonons

Symmetry analysis of the tetragonal structure (D_{4h}^2) of the $\text{La}_{2-x}\text{Sr}_x\text{CuO}_{4-y}$ system ($x \geq 0.10$) indicates that there are seven allowed ($\mathbf{q}=\mathbf{0}$) infrared vibrations: $4E_u$ (x,y symmetry) + $3A_{2u}$ (z symmetry). Unambiguous symmetry assignments to Raman and ir frequencies of materials having lower than cubic symmetry require polarization studies on single-crystal material. Due to the difficulties encountered in producing Sr-doped single crystals with faces large enough to do polarization studies, no single-crystal polarization study of $\text{La}_{2-x}\text{Sr}_x\text{CuO}_{4-y}$ for $\mathbf{E}\parallel\hat{c}$ and $\mathbf{E}\perp\hat{c}$ has yet to our knowledge been carried out.¹⁹

It is therefore useful to tentatively assign frequencies to the allowed ir vibrations of $\text{La}_{2-x}\text{Sr}_x\text{CuO}_{4-y}$ from the present study of polycrystalline pellet samples. By inter-

TABLE I. Fitting parameters (frequencies in cm^{-1}) for $\mathbf{E}\parallel\hat{c}$ and $\mathbf{E}\perp\hat{c}$ polarizations.

Polarization		Sr concentration (x)				
		0	0.05	0.10	0.15	0.20
$\mathbf{E}\parallel\hat{c}$	A_{2u_1} -LO	590	570	575	580	570
	A_{2u_1} -TO	510	515	510	510	505
	A_{2u_2} -LO	465	460	460	455	460
	A_{2u_2} -TO	240	250	230	240	235
	A_{2u_3} -LO					
	A_{2u_3} -TO					
	ω_p^a	~ 0	< 980	< 1100	< 1040	< 1030
	ϵ_{∞}	3	5	5	5	5
$\mathbf{E}\perp\hat{c}$	E_{u_1} -LO	740	720	720		
	E_{u_1} -TO	680	685	685		
	E_{u_2} -LO	450	445	435	420	410
	E_{u_2} -TO	380	380	390	385	380
	E_{u_3} -LO	340	335	345		
	E_{u_3} -TO	160	150	155		
	E_{u_4} -LO					
	E_{u_4} -TO					
	ω_p	< 800 ^b	4900	5500	5200	5150
	γ_p	0	3400	2850	1950	2900
	ϵ_{∞}	3	1	1	1	1

^aEstimated from the anisotropy of the critical fields (see text).

^bThis value represents the upper limit of our uncertainty in ω_p .

TABLE II. Comparison of fitting parameters (frequencies in cm^{-1}) for $\text{La}_{2-x}\text{Sr}_x\text{CuO}_{4-y}$ obtained from data for single-crystal ($x=0.17$) and polycrystalline ($x=0.15$) samples.

Polarization (cm^{-1})	Phonon modes	This work ^a (poly.)	Tajima <i>et al.</i> ^b (single)	Sulewski <i>et al.</i> ^c (poly.)	Schlesinger <i>et al.</i> ^d (poly.)
E \hat{c}	ω_{TO}	240	230	242	240
	ω_{LO}	455		465	
	ω_{TO}	510	510	494	490
	ω_{LO}	580		595	
	ω_p	< 1040	~0	12 100	1300
	γ_p			19 358	3000
	ϵ_∞	5		10.4	4.5
E \perp \hat{c}	ω_{TO}			135	150
	ω_{LO}			150	
	ω_{TO}	385	360	360	350
	ω_{LO}	420		390	
	ω_{TO}			650	680
	ω_{LO}			660	
	ω_p	5200	7180	13 712	13 000
	γ_p	1950	6695	24 198	3000
	ϵ_∞	1	7	1	4.5

^aEffective medium approximation (EMA) calculation with spherical crystallites.

^bExperimental results from E \perp \hat{c} polarized reflectance study of single-crystal $\text{La}_{1.8}\text{Sr}_{0.2}\text{CuO}_4$. The E|| \hat{c} contribution was inferred from comparisons with polycrystalline data (Ref. 14).

^cEMA calculation with rod-shaped crystallites (Ref. 7).

^dLarge crystallite limit approximation (Ref. 8).

preting our ir frequencies in light of optical studies on single-crystal K_2MnF_4 ,^{20,21} Rb_2MnCl_4 ,^{20,21} and La_2NiO_4 ,¹³ which are isomorphic with $\text{La}_{2-x}\text{Sr}_x\text{CuO}_{4-y}$, we have assigned frequencies to the ir-active, zone center vibrations in the D_{4h}^7 space group. In Fig. 2, the displacements and symmetries of the ir-allowed modes of La_2CuO_4 are illustrated using the eigenvectors calculated for the isomorphic K_2MnF_4 by Strobel and Geick.²¹ In Table III, the frequencies of these vibrations are compared with the frequencies of similar vibrations in the isomorphic materials. Table III also lists the phonon frequencies predicted for the tetragonal phase of $\text{La}_{2-x}\text{Sr}_x\text{CuO}_{4-y}$ from reduced mass scalings of similar vibrational frequencies of the isomorphs.

Neither the A_{2u_3} nor E_{u_4} modes are evident in the $\text{La}_{2-x}\text{Sr}_x\text{CuO}_{4-y}$ spectra, because the frequencies of these peaks reside below the spectral range examined.¹⁹ The frequencies of these vibrations in K_2MnF_4 are 158 cm^{-1} and 102 cm^{-1} , respectively. Scaling these values with the reduced masses of $\text{La}_{1.9}\text{Sr}_{0.1}\text{CuO}_4$ yields frequencies of 107 and 66 cm^{-1} , respectively, which are near the long-wavelength limit of our spectrometer. However, it is possible that the frequencies do not simply scale (e.g., because of different Coulombic interactions). To obtain further support for the mode assignments, the frequencies of the A_{2u} and E_u modes identified in our ir spectra were independently calculated by scaling the frequencies of the La_2NiO_4 vibrations, and the results are tabulated in Table III, showing good agreement with the experimental values. Burns *et al.*²² have also assigned symmetries and frequencies to ir phonons of a polycrystalline $\text{La}_{1.85}$ -

$\text{Sr}_{0.15}\text{CuO}_4$ reflectivity spectrum by invoking a similar analogy to Sr_2TiO_4 . The disagreement between the phonon assignments given in this work and in the study reported by Burns *et al.* illustrates the necessity of single-crystal measurements for unambiguous symmetry assignments.

Figure 3 shows the dependence on Sr concentration of the LO and TO E_u (unshaded circles) and A_{2u} (shaded circles) phonon frequencies listed in Table I. The estimated uncertainty in frequency is also shown. No obvious softening of phonon modes with Sr doping is observed. An apparent softening of the low-frequency A_{2u} TO vibration when x is increased from 0 to 0.15 has been reported by Schlesinger *et al.*,⁸ and Tajima and co-workers.¹⁴ Whereas Schlesinger *et al.* assumed this mode to involve La vibrations and the softening was a consequence of the replacement of trivalent La with divalent Sr, Tajima *et al.* proposed that the phonon softens abruptly at the Sr concentration corresponding to the onset of superconductivity and the disappearance of antiferromagnetic order. According to our model, however, the 240 cm^{-1} A_{2u_2} phonon is present in all the spectra, and we see no evidence for the softening of this mode at room temperature.

The E_{u_1} , E_{u_2} , and E_{u_3} modes, which are dominated by the vibrations of in-plane copper and oxygen atoms, decrease in oscillator strength or disappear entirely as the Sr concentration is increased. This is probably due to an increase in the ab plane carrier density and the concomitant electronic screening provided by the Drude response. Substitution of Sr for La produces holes on the in-plane Cu and/or O sites, leading to a quasi-two-dimensional me-

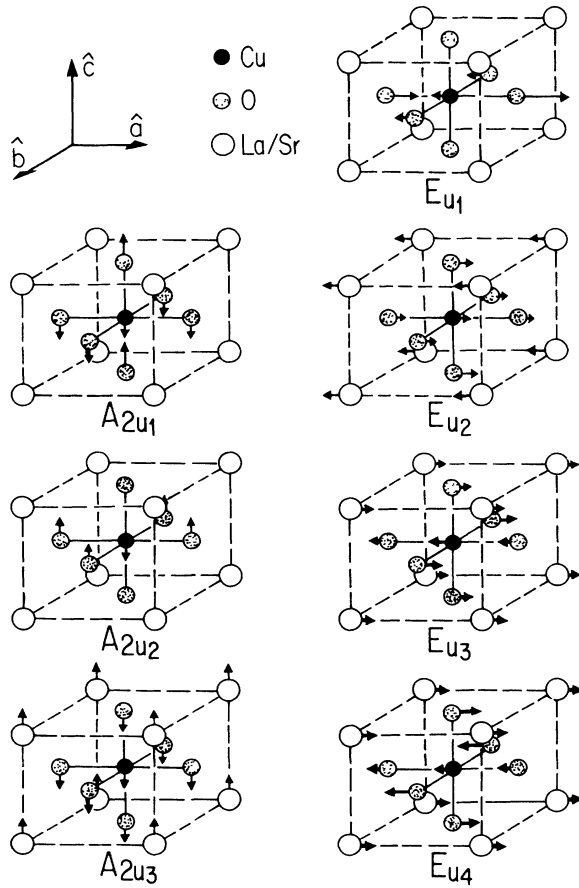


FIG. 2. Normal-mode displacements and assigned symmetries of the allowed $q=0$ ir phonon modes of the D_{4h} space group. The eigenvectors, calculated by Strobel and Geick (Ref. 21) for K_2MnF_4 , show the relative motion of the atoms, which should be suitably modified for the La_2CuO_4 system.

tallic system. The increase in carrier density screens the ir-phonon response. In particular, the modes that are dominated by the motion of the in-plane O^{2-} anions (i.e., E_{u1} and E_{u3}) disappear for x greater than 0.10.

C. Drude parameters

The dependence of the in-plane Drude parameters ω_p and γ_p on Sr concentration deduced from our model is shown in Figs. 4 and 5, respectively. In a band picture, the unscreened plasma frequency is given by

$$\omega_p^2 = \frac{4\pi n e^2}{m_{opt}}, \quad (3)$$

where n is the carrier density, e is the electronic charge, and m_{opt} is the optical band mass expressed in terms of the free-electron mass (m_e). Replacing La^{3+} with Sr^{2+} introduces holes (x) into the system, so n in Eq. (3) becomes x/V_c , where V_c is the volume of the unit cell. In a rigid-band picture, where Sr^{2+} doping lowers E_F without altering the band dispersion, the plasma frequency should

TABLE III. The ir TO phonon frequencies (in cm^{-1}) of $La_{1.9}Sr_{0.1}CuO_{4-y}$ and isomorphic compounds.

	E \hat{c}				E $\perp\hat{c}$		
	A_{2u_3}	A_{2u_2}	A_{2u_1}	E_{u_4}	E_{u_3}	E_{u_2}	E_{u_1}
K_2MnF_4 ^a	158	238	334	102	123	184	421
Rb_2MnF_4 ^a	99	145	209	69	100	119	251
La_2NiO_4 ^b		280	505		150	355	650
$La_{1.9}Sr_{0.1}CuO_4$ (calculated) ^c	107	276	500	66	145	355	646
$La_{2-x}Sr_xCuO_{4-y}$ (from data)		230	510		155	390	685

^aReference 19.

^bReference 13.

^cThe calculated frequencies for the A_{2u_3} and E_{u_4} phonons are derived from scaling phonon frequencies of K_2MnF_4 by the reduced mass of the $La_{2-x}Sr_xCuO_{4-y}$ vibration. All other phonon frequencies were calculated from the La_2NiO_4 values.

be proportional to $x^{1/2}$. The solid line in Fig. 4 denotes the results of a rigid-band calculation with $m_{opt}=2m_e$, and V_c equal to values reported by Hinks *et al.*²³ from neutron diffraction studies on $La_{2-x}Sr_xCuO_4$. Choosing the in-plane m_{opt} in this way forces the calculation through the ω_p ($x=0.05$) experimental result.

A deviation of the experimental plasma frequencies ($x \geq 0.10$) from rigid-band behavior (based upon the above assumptions) is immediately apparent. We are therefore faced with the question of why ω_p deviates from rigid-band behavior as a function of x . In response to this question, Tajima *et al.*² suggested that a saturation in the plasma frequency with Sr doping may be caused by a logarithmic divergence in the density of states at the Fermi level. Another possibility is that a high density of states is pinning the plasma minimum, through the following mechanism. Sr doping lowers the Fermi energy (E_F) which for $x=0$ lies in an oxygen $2p_{x,y}$ band due to the large electronic anisotropy of the material. As the Sr concentration x is increased, E_F is lowered until it encounters

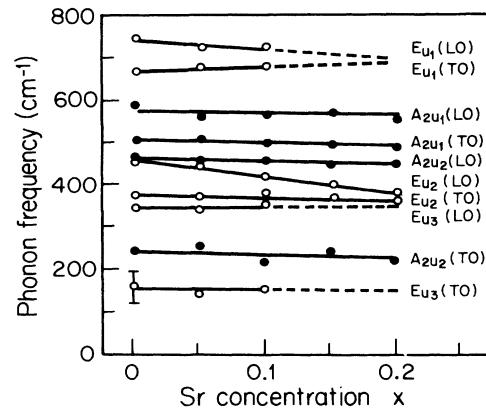


FIG. 3. Frequencies of the ir-active phonons in $La_{2-x}Sr_xCuO_{4-y}$ plotted vs x . Damping due to electronic screening effects is observed for the E_u modes, which involve the in-plane motion of the oxygen anions.

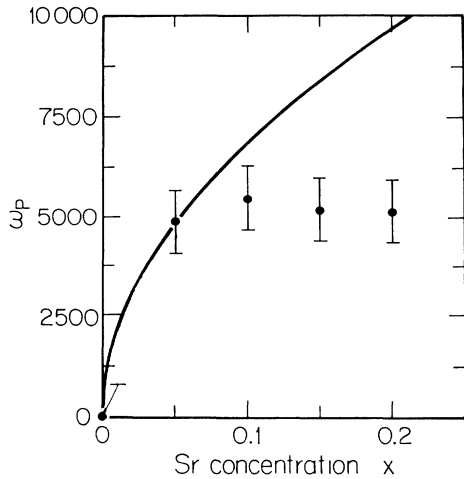


FIG. 4. Plasma frequencies (ω_p) obtained from the fits to the reflectance data plotted vs Sr concentration (x). An estimated error ($\pm 800 \text{ cm}^{-1}$) is shown. The solid line represents a rigid-band calculation of ω_p assuming $m_{\text{opt}} = 2m_e$.

a Cu $3d$ band. We suggest that the narrowness and large optical band mass of the Cu $3d$ band pins E_F and hence ω_p . From our data in Fig. 4, this pinning would occur for $x > 0.05$. Support for the placement of E_F in an O $2p$ band for oxygen-deficient La_2CuO_4 is provided by spectroscopic measurements^{24,25} and by the relatively low optical band mass ($m_{\text{opt}} = 2m_e$) deduced for $x \leq 0.05$.

For the polycrystalline samples, the out-of-plane plasma frequency (ω_p^{\parallel}) cannot be measured directly. However, estimates for $\omega_p^{\parallel}(x)$ can be made by relating the band masses to results of critical-field measurements on similar samples. The critical-field anisotropy ratio in the high- T_c copper oxides is estimated to be ~ 5 . Based on the Ginzburg-Landau theory, the square of this ratio is proportional to the mass anisotropy (m_{\parallel}/m_{\perp}). Placing this mass anisotropy in the expression for the optical plasma frequency, we find $\omega_p^{\parallel} \sim \frac{1}{5} \omega_p^{\perp}$ for $x \geq 0.05$, and the values

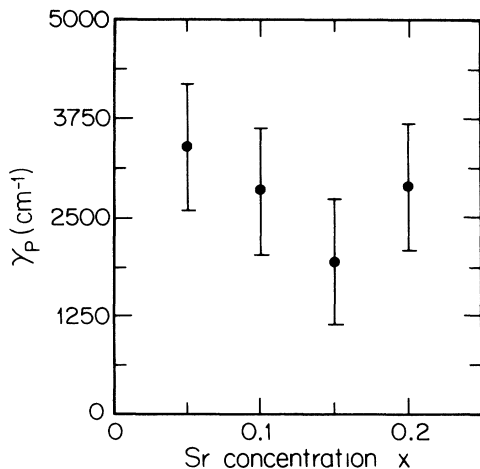


FIG. 5. Plasma damping factor (γ_p) obtained from the fits to the reflectance data plotted vs Sr concentration (x).

of $\omega_p^{\parallel}(x)$ estimated in this manner are given in Table I.

The minimum in γ_p that occurs at $x = 0.15$ (see Fig. 5) indicates that the carrier lifetime is longest for this Sr concentration, which also yields the highest T_c values for the $\text{La}_{2-x}\text{Sr}_x\text{CuO}_{4-y}$ system. We found in this work that the room-temperature reflectance spectra of $\text{La}_{2-x}\text{Sr}_x\text{CuO}_{4-y}$ can be adequately described with a frequency-independent carrier lifetime. Recently, a frequency-dependent carrier lifetime analysis was used to interpret the far-ir optical spectra of the $\text{YBa}_2\text{Cu}_3\text{O}_7$ material in the region of the proposed superconducting gap as was also applied in similar studies to some of the heavy fermion systems.²⁶ This approach is justified if a simple Drude model clearly does not fit the data. However, a frequency-dependent free-carrier mass is not proved in this approach, since another loss mechanism (i.e., low-frequency phonons, etc.) may be responsible for the inability to fit the data at low energy to a Drude form.

A comparative study of the dc conductivity deduced from the optical measurements ($\sigma_0 = \omega_p^2 \tau / 4\pi$) and the direct resistively measured dc conductivity (σ_{dc}) on the same set of samples is shown in Fig. 6. Good agreement is obtained between these independent measurements of σ_0 and σ_{dc} , indicating that the Drude parameters obtained from our model provide consistent estimates for the optical conductivity of the ab planes, and for the large anisotropy in σ_{dc} (parallel and perpendicular to the ab planes).

The frequency dependent conductivity $\sigma(\omega)$ derived by Herr *et al.*¹ from a Kramers-Kronig analysis of the polycrystalline reflectance spectra has a strong absorption at 240 cm^{-1} . This feature was later labeled a "charged phonon" by Rice and Wang.²⁷ Based on the results of this study and the single-crystal study of Tajima *et al.*,¹⁴ it appears that the feature which gave rise to the proposed 240-cm^{-1} charged phonon is completely explained by the anisotropy analysis in terms of a dominant A_{2u} mode so that the previous misidentification is due to the improper treatment of the optical anisotropy.

The appearance of a 0.4-eV peak in the Kramers-

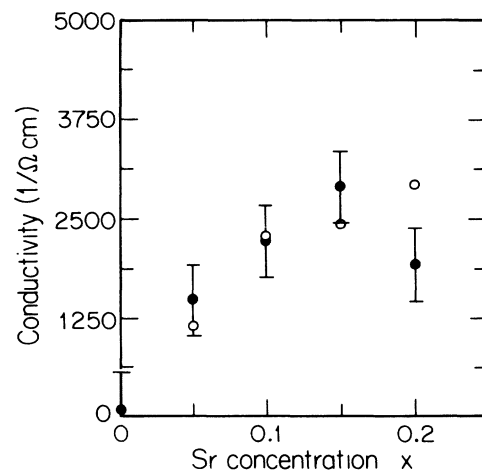


FIG. 6. dc conductivity obtained from the optical measurements $\sigma_0 = \omega_p^2 \tau / 4\pi$ (\bullet) and directly (resistively) measured conductivity σ_{dc} (\circ) plotted vs Sr concentration at room temperature.

Kronig conductivity spectra^{1,11} of polycrystalline $\text{La}_{2-x}\text{Sr}_x\text{CuO}_4$ and $\text{YBa}_2\text{Cu}_3\text{O}_{7-\delta}$ samples has been linked²⁷ to a combined excitonic and charged-phonon mechanism for high- T_c superconductivity. However, $E \perp \hat{c}$ spectra for single-crystal $\text{La}_{1.8}\text{Sr}_{0.2}\text{CuO}_4$ (Tajima *et al.*¹⁴) and oriented films of $\text{YBa}_2\text{Cu}_3\text{O}_{7-\delta}$ (Bozovic *et al.*²⁸) clearly show no 0.4-eV feature in that polarization. Whereas these studies cannot completely exclude the possibility of a 0.4-eV feature in the $E \parallel \hat{c}$ spectrum, we have fit out data very well over an extended energy range without the necessity of incorporating any electronic oscillators in this frequency range. Thus, it appears likely that there is not a strong electronic excitation at 0.4 eV in these samples. Since a strong 0.4-eV feature has only been observed in cases where Kramers-Kronig transforms of polycrystalline reflectance spectra have been applied, we conclude that this feature may be a by-product of failing to consider the anisotropy properly.

IV. CONCLUSIONS

Since it has been difficult to produce large single crystals of $\text{La}_{2-x}\text{Sr}_x\text{CuO}_{4-y}$ with $0.05 \leq x \leq 0.20$ (the range of x yielding the high- T_c values), optical studies examining the superconducting state have necessarily been performed on polycrystalline pellet samples. The results of the present study on the normal state of these polycrystalline samples are of importance in understanding the electronic as well as the lattice properties of the superconducting state. In this work, the effect of the crystalline anisotropy on the lattice and electronic properties has been studied for $0 \leq x \leq 0.20$. Frequencies of the ir-active phonons were assigned to the vibrational modes of D_{4h}^{17} symmetry, and electronic screening of in-plane oxygen vibrations was observed. We find that the replacement of La^{3+} with Sr^{2+} produces a quasi-two-dimensional metallic system, consistent with the formation of holes on the in-plane Cu and/or O sites, and the increase in the carrier density was

found to screen the ir-phonon response, especially those modes that are dominated by the motion of the in-plane O^{2-} anions. In our analysis, the dependence of the plasma frequency on Sr concentration could be explained by the Fermi energy passing through an $\text{O } 2p_{x,y}$ band as a result of Sr doping and becoming pinned in a Cu $3d$ band for $x > 0.05$.

Single crystals with a faces large enough to support optical polarization studies have recently been produced for $x = 0$ and are currently being examined.²¹ However, the superconducting transitions are generally much broader in single crystals than in the polycrystalline pellets over the appropriate range of x values. This increased broadening is presumably closely related to the greater difficulty in obtaining nearly stoichiometric oxygen concentrations. In this respect, many critical experiments are best performed with the polycrystalline pellet samples, which are more nearly stoichiometric than the corresponding single crystals.²⁹ The results of the present study should, therefore, have relevance to electronic, magnetic, and optical studies on the polycrystalline cuprates.

ACKNOWLEDGMENTS

We are grateful to E. J. Delaney of Lincoln Laboratory for preparing the polycrystalline pellets, J. R. Martin of the MIT Center for Materials Science and Engineering for his assistance in the SEM and Auger measurements, and Professor R. J. Birgeneau, Professor M. A. Kastner, Dr. J. Steinbeck, and Ms. A. Chaiken for valuable discussions. This work was supported at MIT by the National Science Foundation on Materials Research Laboratory Grant No. DMR87-19217 (initially) and by the Air Force of Scientific Research Grant No. 88-0021 (subsequently), and at MIT Lincoln Laboratory by the Department of the Air Force.

¹S. L. Herr, K. Kamarás, C. D. Porter, M. G. Doss, D. B. Tanner, D. A. Bonn, J. E. Greedan, C. V. Stager, and T. Timusk, *Phys. Rev. B* **36**, 733 (1987).

²S. Tajima, S. Uchida, S. Kanbe, K. Kitazawa, K. Fueki, and S. Tanaka, *Jpn. J. Appl. Phys.* **26**, L432 (1987).

³P. E. Sulewski, A. J. Sievers, R. A. Buhrman, J. M. Tarascon, L. H. Greene, and W. A. Curtin, *Phys. Rev. B* **35**, 8829 (1987).

⁴Z. Schlesinger, R. T. Collins, and M. W. Shafer, *Phys. Rev. B* **35**, 7232 (1987).

⁵G. A. Thomas, A. J. Millis, R. N. Bhatt, R. J. Cava, and E. A. Reitman, *Phys. Rev. B* **36**, 736 (1987).

⁶J. Orenstein, G. A. Thomas, D. H. Rapkine, C. G. Bethea, B. F. Levine, R. J. Cava, E. A. Reitman, and D. W. Johnson, Jr., *Phys. Rev. B* **36**, 729 (1987).

⁷P. E. Sulewski, T. W. Noh, J. T. McWhirter, and A. J. Sievers, *Phys. Rev. B* **36**, 5735 (1987).

⁸Z. Schlesinger, R. T. Collins, M. W. Shafer, and E. M. Engler, *Phys. Rev. B* **36**, 5275 (1987).

⁹G. L. Doll, J. Steinbeck, G. Dresselhaus, M. S. Dresselhaus, A. J. Strauss, and H. J. Zeiger, *Phys. Rev. B* **36**, 8884 (1987).

¹⁰G. L. Doll, J. Steinbeck, M. S. Dresselhaus, G. Dresselhaus, A. J. Strauss, H. J. Zeiger, G. Phillips, and J. Waldman, in *High Temperature Superconductors*, edited by M. B. Brodsky, R. C. Dynes, K. Kitazawa, and H. L. Tuller (Materials Research Society, Pittsburgh, 1988), Vol. 99, p. 841.

¹¹S. Etemad, D. E. Aspnes, P. Barboux, G. W. Hull, M. K. Kelly, J. M. Tarascon, R. Thompson, S. L. Herr, K. Kamarás, C. D. Porter, and D. B. Tanner, in Ref. 10, p. 135.

¹²H. P. Gesserich, G. Scheiber, and B. Renker, *Solid State Commun.* **63**, 657 (1987).

¹³J. Bassat, P. Odier, and F. Gervais, *Phys. Rev. B* **35**, 7126 (1987).

¹⁴S. Tajima, S. Uchida, H. Ishii, H. Takagi, and S. Tanaka, *Physica B* (to be published).

¹⁵J. S. Speck, G. L. Doll, M. S. Dresselhaus, G. Dresselhaus, A. J. Strauss, and H. J. Zeiger, *Bull. Am. Phys. Soc.* **33**, 648 (1988).

¹⁶T. Fujita and Y. Maeno, in *Superconducting Materials*, edited by S. Nakajima and H. Fukuyama (Academic, New York, 1988), p. 34.

¹⁷F. Gervais, in *Infrared and Millimeter Waves*, edited by K. J.

- Button (Academic, New York, 1983), p. 306.
- ¹⁸F. Wooten, *Optical Properties of Solids* (Academic, New York, 1972).
- ¹⁹P. C. Eklund, A. M. Rao, G. W. Lehman, G. L. Doll, M. S. Dresselhaus, P. J. Picone, D. R. Gabbe, H. P. Jenssen, and G. Dresselhaus, *J. Opt. Soc.* (to be published).
- ²⁰H. Bürger, K. Strobel, R. Geick, and W. Müller-Lierheim, *J. Phys. C* **9**, 4213 (1976).
- ²¹K. Strobel and R. Geick, *J. Phys. C* **9**, 4223 (1976).
- ²²G. Burns, F. H. Dacol, G. Kliche, W. König, and M. W. Shafer, *Phys. Rev. B* **37**, 3381 (1988).
- ²³D. G. Hinks, B. Dabrowski, K. Zhang, C. U. Segre, J. D. Jorgensen, L. Soderholm, and M. A. Beno, in Ref. 10, p. 9.
- ²⁴Z. Shen, J. W. Allen, J. J. Yeh, J. S. Kang, W. Ellis, W. Spicer, I. Lindau, M. B. Maple, Y. D. Dalichaouch, M. S. Torikachvili, J. Z. Sun, and T. H. Geballe, *Phys. Rev. B* **36**, 8414 (1987).
- ²⁵J. M. Tranquada, S. M. Heald, and A. R. Moodenbaugh, *Phys. Rev. B* **36**, 5263 (1987).
- ²⁶M. Capizzi, J. Orenstein, G. A. Thomas, D. Rapkine, J. P. Remeika, A. S. Cooper, R. J. Cava, and E. A. Reitman, *Bull. Am. Phys. Soc.* **33**, 416 (1988).
- ²⁷M. J. Rice and Y. R. Wang, *Phys. Rev. B* **36**, 8794 (1987).
- ²⁸I. Bozovic, D. Kirillov, A. Kapitulnik, K. Char, M. R. Hahn, M. R. Beasley, T. H. Geballe, Y. H. Kim, and A. J. Heeger, *Phys. Rev. Lett.* **59**, 2219 (1987).
- ²⁹P. J. Picone, H. P. Jenssen, and D. R. Gabbe, *J. Cryst. Growth* **85**, 576 (1987).